Biogeosciences Discuss., 9, 15237–15277, 2012
www.biogeosciences-discuss.net/9/15237/2012/
doi:10.5194/bgd-9-15237-2012

Biogeosciences Discussions

Analysis of a 39-yr continuous atmospheric CO_2 record from Baring Head, New Zealand

B. B. Stephens[1,2], G. W. Brailsford[1], A. J. Gomez[3], K. Riedel[1], S. E. Mikaloff Fletcher[1], S. Nichol[1], and M. Manning[3]

[1]National Institute of Water and Atmospheric Research, Wellington, New Zealand
[2]National Center for Atmospheric Research, Boulder, Colorado, USA
[3]Victoria University, Wellington, New Zealand

Received: 15 September 2012 – Accepted: 10 October 2012 – Published: 31 October 2012

Correspondence to: B. B. Stephens (stephens@ucar.edu)

Published by Copernicus Publications on behalf of the European Geosciences Union.

Abstract

We present an analysis of a 39-yr record of continuous atmospheric CO_2 observations made at Baring Head, New Zealand, filtered for steady CO_2 mole fractions during southerly wind conditions. We discuss relationships between variability in the filtered CO_2 time series and regional to global carbon cycling. Baring Head is well situated to sample air that has been isolated from terrestrial influences over the Southern Ocean, and experiences extended periods of strong southerly winds with low CO_2 variability. The filtered Baring Head CO_2 record reveals an average seasonal cycle with amplitude of 0.95 ppm that is 13 % smaller and 3 weeks earlier in phase than that at the South Pole. Seasonal variations in a given year are sensitive to the timing and magnitude of the combined influences of Southern Ocean CO_2 fluxes and terrestrial fluxes from both hemispheres. The amplitude of the seasonal cycle varies throughout the record, but we find no significant long-term seasonal changes with respect to the South Pole. Interannual variations in CO_2 growth rate in the Baring Head record closely match the El Niño/Southern Oscillation, reflecting the global reach of CO_2 mole fraction anomalies associated with this cycle. We use atmospheric transport model results to investigate contributions to seasonal and annual-mean components of the observed CO_2 record. Long-term trends in mean gradients between Baring Head and other stations are predominately due to increases in Northern-Hemisphere fossil-fuel burning and Southern Ocean CO_2 uptake, for which there remains a wide range of future estimates. We find that the postulated recent reduction in the efficiency of Southern Ocean anthropogenic CO_2 uptake as a result of increased zonal winds is too small to be detectable as significant differences in atmospheric CO_2 between mid- to high-latitude Southern Hemisphere observing stations.

BGD

9, 15237–15277, 2012

1 Introduction

The future trajectory of carbon exchange between the atmosphere and the Earth's oceans and terrestrial ecosystems remains a primary uncertainty in climate projections (IPCC, 2007). Predicting the response of global carbon fluxes to expected changes in atmospheric CO_2, temperature, precipitation, and surface winds requires a better understanding of how and why these fluxes vary on synoptic to decadal timescales (Friedlingstein et al., 2006; Le Quéré et al., 2007; Zickfeld et al., 2008), which in turn requires long-term, high-quality, and globally distributed observations of atmospheric CO_2 mole fractions (Keeling, 1961; Keeling et al., 2001; Rödenbeck et al., 2003; Gurney et al., 2008; Patra et al., 2008).

As the primary area for the exchange of heat and gases between recently upwelled surface waters and the atmosphere, the Southern Ocean is a region of critical importance for future climate change and atmospheric CO_2 (Sarmiento et al., 1998; Caldeira and Duffy, 2000). However, the Southern Ocean's response to climate change depends on complex interactions between biogeochemical and dynamic processes, and the net feedback on anthropogenic CO_2 uptake will be mediated by varying influences associated with changes in solubility, biological, and anthropogenic forcing (Sarmiento et al., 1998; Caldeira and Duffy, 2000; Zickfeld et al., 2008; Lovenduski and Ito, 2009). Observations over the past several decades have suggested a significant poleward intensification and strengthening of Southern Ocean winds (Thompson and Solomon, 2002; Marshall, 2003), yet it is unclear what effect these changes are having on deep-water ventilation (Saenko et al., 2005; Böning et al., 2008) or what effect ventilation changes may be having on air-sea CO_2 fluxes (Wetzel et al., 2005; Le Quéré et al., 2007; Lovenduski et al., 2007; Law et al., 2008; Zickfeld et al., 2008; Lenton et al., 2009; Lovenduski and Ito, 2009; Takahashi et al., 2009).

Long-term atmospheric CO_2 records at mid to high southern latitudes have significant potential to shed light on past and ongoing changes in Southern Ocean CO_2 fluxes. However, the available records are few and regional background CO_2 gradients

BGD
9, 15237–15277, 2012

induced by changes in the Southern Ocean carbon sink are small, which makes their interpretation by atmospheric transport models challenging (Law et al., 2003, 2008). As a consequence, the available records are important and should be examined closely to improve their compatibility across the global network and to maximize their scientific utility through data-based analyses.

One of the longest CO_2 records comes from Baring Head, New Zealand (BHD), where continuous instruments have recorded measurements since 1972 (Lowe et al., 1979; Manning and Pohl, 1986; Manning et al., 1994; Brailsford et al., 2012) and are currently operated by staff of the New Zealand National Institute of Water and Atmospheric Research (NIWA). These data have been used in studies investigating the global carbon cycle and in community data synthesis products (e.g. Keeling et al., 1989a, 2001; Gurney et al., 2002; Le Quéré et al., 2007; WDCGG, 2012; Globalview-CO_2, 2011). There are relatively few atmospheric CO_2 observing sites in the Southern Hemisphere, and most of these are flask collection sites lacking in situ instrumentation. As a result, the Baring Head record is uniquely valuable for addressing questions about interannual variability and trends for the carbon cycle at high southern latitudes and globally. Lowe et al. (1979) discussed the results from the first four years of this dataset, describing the secular trend and seasonal cycle. Here, we present a newly re-processed version of the full dataset and its variability with respect to other stations and important climate processes. A companion paper details the history of the site, measurement techniques, calibration methodology, and intercomparison results (Brailsford et al., 2012).

To aid interpretation of the Baring Head CO_2 time series and provide clues to sources of the observed trends and variability, we include measurements from the Scripps Institution of Oceanography (SIO) CO_2 program made on flasks collected at the South Pole (SPO) and by in situ instrumentation at Mauna Loa Observatory in Hawaii (MLO) (Keeling et al., 2001). The high time resolution of the Baring Head data allows for robust identification of background mole fractions as well as analyses of synoptic scale processes. In this paper, we focus on the interpretation of measurements that have been

BGD
9, 15237–15277, 2012

A 39-yr atmospheric CO_2 record from Baring Head, New Zealand

B. B. Stephens et al.

filtered to sample during steady CO_2 conditions when air is arriving from the high-latitude Southern Ocean. Aspects of the regional information contained in short-term variations will be the focus of subsequent research. In Sect. 2 we summarize the Baring Head site characteristics, including information on the origins of air masses arriving at the site and the selection criteria for steady periods. In Sect. 3, we analyze and discuss annual mean mole fractions, seasonal and interannual variations, and long-term trends in the CO_2 time series and their relationship to Southern Ocean and global carbon exchanges.

2 Background

2.1 Site location and air origins

In 1970, in conjunction with the Department of Scientific and Industrial Research (DSIR, predecessor to NIWA) in New Zealand, C.D. Keeling's group from SIO established an NDIR analyser at Makara (41°15′ S, 174°41′ E) about 15 km northwest of Wellington and 1 km inland from the west coast of the North Island, New Zealand (Fig. 1a). However, the first 1.5 yr of measurements at this site suggested that it was too strongly influenced by local terrestrial signals, and the analyzer was moved to Baring Head (41°25′ S, 174°52′ E) in December 1972. The measurements of atmospheric CO_2 at the Baring Head site have continued to the present, making it the longest running in situ atmospheric CO_2 observing station in the Southern Hemisphere.

Baring Head is located approximately 10 km southeast of the city of Wellington (Fig. 1a). The measurement system is housed in a concrete building close to the edge of a coastal cliff with a southerly aspect. A pair of air intakes is located 10 m above the adjacent ground level, 85 m above mean sea level, and approximately 240 m from the ocean. The intervening land consists of a beach strip and cliff face containing sparse, shrubby vegetation. There is a single residence to the north of the site; otherwise, there is no permanent occupation within 3 km. The surrounding land has been used

BGD
9, 15237–15277, 2012

fairly consistently for low density livestock farming. The Wellington city area has a population of approximately 380 000. The station is visited by NIWA staff for maintenance of equipment on a weekly schedule.

Baring Head was chosen to make CO_2 measurements representative of large relatively homogeneous Southern Ocean air masses. Wind speeds at the site are typically high, reducing the impacts of local sources. Also, southerly air arriving at this site has often been out of contact with terrestrial sources and sinks of CO_2 for thousands of km, having travelled over the Southern Ocean between the latitudes of 45 and 70° S for the preceding week or more. These characteristics provide ideal conditions for determining baseline levels of atmospheric CO_2 at these latitudes, but at other times the site receives air that has recently passed over New Zealand or Australia. Figure 1b shows the results of a clustering analysis on 20 yr of 4-day back trajectories for air arriving at Baring Head. The back trajectories were calculated every 12 h using the method of Gordon (1986) driven by winds from the New Zealand Meteorological Service primitive equation model.

Onshore winds are usually associated with a repeating synoptic pattern in which an anticyclone moves from the Tasman Sea, to the west of New Zealand, onto the country modulating the background westerly winds (Kidson, 2000). The Southern Alps of the South Island of New Zealand, which reach a height of 3750 m, have a major effect on air flow throughout the region. When the centre of an anticyclone is well to the west of New Zealand, the mountain range acts to deflect air flow northward along the west coast of the South Island and then through the Cook Strait separating the North and South Islands. This results in a northwest wind in the strait that is further channelled by topography to a local wind at Baring Head that is from the north. As the anticyclone moves eastward, a transition occurs to a regime in which air flows around the south of the South Island, and the local wind at Baring Head is from the south. This synoptic pattern is typically associated with a descending air mass and back trajectories that come from around 55° S and have not crossed land in at least 4 days. As the clustering analysis in Fig. 1b indicates, south- and southeast-arriving

BGD
9, 15237–15277, 2012

trajectories occur approximately 27 % of the time. Southerly wind events can persist for several days at a time and occur roughly 4 times per month in winter and 2 times per month in summer.

2.2 Data filtering

Isolating clean marine background measurements from those influenced by local terrestrial fluxes requires a data filtering scheme informed by a good knowledge of the local site and wind conditions and their influence on CO_2 variability. As discussed above, the topography of the South Island, Cook Strait, and the mountains near Baring Head result in the site almost exclusively experiencing due northerly or due southerly winds that are often quite strong. Figure 2a shows frequency distributions for winds of different directions and speed. As this figure indicates, approximately 2 / 3 of the time the hourly average wind direction is within 30 degrees of north, and 1 / 2 of these winds are over $10\,m\,s^{-1}$. The remaining 1 / 3 of the time, the wind is primarily from the south, with 2 / 3 of these winds over $10\,m\,s^{-1}$ and the stronger winds holding closer to due south.

These wind conditions have a major influence on CO_2 variability, with hourly standard deviations less than 0.2 ppm corresponding to strong northerlies and moderate southerlies, and higher variability to weak winds and moderate northerlies (Fig. 2b). Although strong northerlies are often associated with low CO_2 variability, it is apparent from comparing mole fractions measured during these periods to those during southerlies that they still reflect significant terrestrial influences. Figure 2c, d shows that these strong northerlies are typically around 0.5 ppm lower in CO_2 during day, and 0.5 ppm higher during night as a result of upwind photosynthesis and respiration on the North Island. High daytime CO_2 mole fractions during infrequent weak westerlies likely result from emissions associated with the large populations in the city of Wellington and surrounding suburbs.

In order to obtain a baseline record representative of large marine air masses, we have employed a filter focused on retrieving long periods of steady CO_2 mole fractions when air arrived from the south without first crossing over the South Island (see Fig. 1).

BGD
9, 15237–15277, 2012

We start with a multi-step filter in which first “steady intervals” for either of two inlet lines are defined as intervals for which the CO_2 mole fraction has a maximum standard deviation of 0.1 ppm for a minimum length of 6 h. Then, overlapping steady intervals for one or both inlet lines are aggregated into “steady periods,” which can themselves have slowly trending mole fractions. Next, these steady periods are further screened to exclude cases when the wind was not from the south, and finally they are also screened to exclude cases when it is likely the air passed over the South Island before arriving at Baring Head. This last step is accomplished by requiring that the atmospheric pressure difference across the Southern Alps, as measured by the difference between pressure at Christchurch on the east coast and that at Hokitika on the west coast (Fig. 1a), be 1 mbar or greater averaged over the steady period (Manning and Pohl, 1986).

Prior to March of 1978, steady period selection was done manually on the basis of consecutive 30-min averages having a range less than 0.1 ppm, and including the southerly criteria but not the Christchurch–Hokitika pressure difference. Using the newer filter criteria over the 33 yr since then, steady periods have been found to occur on average 36 times per year, last on average 17 h, and constitute 13 % of the complete observational record. This is significantly less than the percentage of southerly conditions because of the requirement for the conditions to persist for 6 h. There is significant seasonal variability in the occurrence of steady periods and also some in their duration, with 67 % more periods, totalling twice as much overall time, occurring in the winter months of June–August compared to the summer months of December–February. The southerly criterion excludes 13 % of steady CO_2 periods, but less than 8 % in terms of time as the northerly steady CO_2 periods tend to be shorter. The Christchurch–Hokitika pressure difference excludes another 26 % of the remaining steady periods and 18 % in terms of time. Each of the resulting filtered steady periods is treated as a unique single event, and CO_2 data reported to community data collections (Globalview-CO_2, 2011; WDCGG, 2012) have historically consisted of average mole fractions, standard deviations, start times, and durations for each steady period. Figure 3 shows both the unfiltered and filtered CO_2 time series for Baring Head. The smoothness of the

BGD
9, 15237–15277, 2012

A 39-yr atmospheric CO_2 record from Baring Head, New Zealand

B. B. Stephens et al.

steady period curve relative to the scatter of all hourly averages reveals the power of this filtering method to isolate remote marine signals. Simple filters based on hourly wind direction or within hour CO_2 variability are much less selective. The frequency of steady periods found has varied from year to year. Although this may be the result of changes in atmospheric transport patterns or variable CO_2 fluxes, variations in the number of steady periods could also be related to changes in instrument procedures or performance (Brailsford et al., 2012).

We employ the detailed filter criteria to enable time-series analysis on low-variability background marine air and to investigate questions about changes in Southern Ocean fluxes. Coarse-resolution models that use these steady-period Baring Head data or synthesized products based on them (Globalview-CO_2, 2011) must account for this filtering to adequately represent the observing conditions. Recognizing the ability of more recent models to combine higher resolution data with information on corresponding synoptic transport in order to infer fluxes on regional scales, we also make the hourly mean unfiltered CO_2 time series publicly available, along with values for short-term variability and winds.

3 Results

3.1 Time series

Salient features of the long-term steady-period record include (1) a long-term growth rate of approximately 1.5 ppm yr^{-1} driven by global fossil-fuel consumption and deforestation, (2) annual-mean differences with respect to other stations consistent with fossil-fuel burning in the Northern Hemisphere and oceanic CO_2 uptake in the Southern Hemisphere, (3) a seasonal cycle of around 1 ppm amplitude related to ocean exchange in the Southern Hemisphere and the influence of terrestrial fluxes in both the Northern and Southern Hemispheres, (4) interannual variations in the long-term growth rate reflecting global and Southern Ocean carbon cycle processes, and (5) long-term

Discussion Paper | Discussion Paper | Discussion Paper | Discussion Paper |

BGD
9, 15237–15277, 2012

A 39-yr atmospheric CO_2 record from Baring Head, New Zealand

B. B. Stephens et al.

trends in differences from other stations which have the potential to constrain trends in Southern Ocean CO_2 fluxes.

To visually decompose the variations on different time scales, we use the seasonal time-series decomposition by Loess (STL) routine (Cleveland and McRae, 1989; Cleveland et al., 1990), which allows for changes in seasonal patterns over time. This routine fits locally weighted polynomial regressions to time series composed of all values from individual months, for example all average January values for the entire record, as well as the remaining deseasonalized trend, in an iterative process. The degrees to which the seasonal cycle and long-term trend are allowed to vary to fit the data are set by specifying the window for the seasonal and trend Loess fits. We use a seasonal cycle window of 5 yr and first run the procedure using a trend window of 121 months intended to reflect changes on decadal timescales. Then, after removing this component we run the procedure again with a trend window of 25 months to capture subdecadal components. Figure 4 shows the results of this STL calculation for Baring Head. We have run the same routine and parameters on South Pole flask and Mauna Loa continuous data from SIO for the overlapping time period.

3.2 Annual-mean mole fractions

Averaged over the entire 39-yr record, the difference between Baring Head and Mauna Loa (BHD-MLO) is −2.30 ppm, and the difference between Baring Head and the South Pole (BHD-SPO) is 0.05 ppm. For the decade 2000–2009, the average BHD-MLO difference is −3.03 ppm and the average BHD-SPO difference is −0.05 ppm. The Baring Head record exhibits increasingly lower mole fractions than Mauna Loa because of the predominance and growth of fossil fuel CO_2 emissions in the Northern Hemisphere and oceanic CO_2 uptake in the Southern Hemisphere. Despite being further north than the South Pole, Baring Head shows similar and trending lower annual-mean CO_2 mole fractions. This reflects the greater influence of the increasing Southern Ocean CO_2 sink on air at Baring Head (Keeling et al., 1989b; Kawa et al., 2004).

BGD
9, 15237–15277, 2012

In order to explore the relative roles that sources and sinks from different geographic regions play in forming spatial and temporal variations in atmospheric CO_2 related to Baring Head, we have run the fine resolution version of the TM3 transport model, which has a resolution of $\sim 3.8^\circ$ latitude by 5° longitude with 19 vertical levels (Heimann and Körner, 2003). This model was forced by ECMWF winds and CO_2 sources and sinks from CarbonTracker 2010 (Peters et al., 2007) over the period 2000–2009. In order to be able to isolate the influence of different regions and source processes on the station, fossil-fuel emissions, biomass burning, the terrestrial biosphere, and the oceans were each treated as separate tracers in the model and separated geographically according to the TransCom flux regions (Gurney et al., 2003). To determine the modelled sensitivity at a particular station to a particular source, we divide the corresponding CO_2 signal, averaged over the period 2003–2009 to allow 3 yr for model spin-up, by the corresponding source strength. The resulting sensitivities are similar to those found with other atmospheric transport models (Gurney et al., 2003). For our calculations, we extract CO_2 values at a point 1000 km to the southwest of Baring Head (50° S 170° E, see Fig. 1), to represent the steady-period Baring Head record, as the modelled values for Baring Head used no filtering for steady-CO_2 southerly wind conditions.

The TM3 model CO_2 sensitivities, scaled by the 2000–2009 fossil-fuel source, results in an average BHD-MLO difference of −4.57 ppm and an average BHD-SPO difference of 0.17 ppm. The TM3 model sensitivities suggests that a postulated 0.3 Pg C yr^{-1} sink in the high-latitude Southern Ocean (Gruber et al., 2009) results in a −0.38 ppm BHD-MLO difference and a −0.13 ppm BHD-SPO difference. Furthermore, the model sensitivities predict that a plausible 1.1 Pg C yr^{-1} sink in the temperate Southern Hemisphere oceans (Gruber et al., 2009) results in a −0.87 ppm BHD-MLO difference and a −0.07 ppm BHD-SPO difference. Although southern temperate ocean fluxes have relatively small influences on the annual mean BHD-SPO differences, because atmospheric transport generates phase differences, they can have a larger effect on monthly site differences (see next section). Tropical and Northern Hemisphere terrestrial biosphere and ocean fluxes are responsible for countering the influence of the fossil-fuel

BGD
9, 15237–15277, 2012

source and Southern Ocean sink on the BHD-MLO gradient, to produce the observed value (−3.03 ppm), but their relative proportion is model-dependent and a topic of active research (Stephens et al., 2007). TM3 and other models suggest that tropical and northern fluxes have little influence on the BHD-SPO differences. The counteraction of the fossil-fuel source and Southern Ocean sinks described above can explain the observed 2000–2009 annual-mean BHD-SPO difference (−0.03 model vs. −0.05 observed) well within the limits of uncertainty.

3.3 Seasonal cycles

Figure 5 shows the average seasonal cycles at Baring Head, for steady period data, and at South Pole for the 39-yr period of the Baring Head record. The amplitude of the average Baring Head cycle is 0.95 ppm with a late-winter maximum in September, and an early-autumn minimum in March. This cycle is 13 % smaller and 3 weeks earlier in phase compared to that at the South Pole. Both cycles are small relative to those at Northern Hemisphere stations, but their timing and amplitudes may represent important tests for our understanding of hemispheric CO_2 fluxes and interhemispheric atmospheric transport (Dargaville et al., 2003; Baker et al., 2006).

Early studies recognized that seasonal cycles in atmospheric CO_2 at high southern latitudes represented the combined influences of Northern Hemisphere terrestrial fluxes delayed by interhemispheric transport and Southern Hemisphere terrestrial and oceanic fluxes (Pearman and Hyson, 1980; Heimann et al., 1989) but lacked sophisticated estimates of these processes. More recent models of atmospheric CO_2 at high southern latitudes incorporate improved knowledge of flux distributions and better transport, but still show differences in relative seasonal contributions at high southern latitudes (Heimann et al., 1998; Erickson et al., 1996; Gurney et al., 2004; Roy et al., 2003; Takahashi et al., 2009; Dargaville et al., 2002; Nevison et al., 2008). However, the general picture for the Baring Head record has remained relatively consistent over time, in which the influence from Northern Hemisphere terrestrial fluxes is lagged by

BGD
9, 15237–15277, 2012

approximately 6 months and reduced such that it is comparable in phase and magnitude to that from Southern Hemisphere terrestrial fluxes (Heimann et al., 1989, 1998).

Figure 6 shows model-estimated contributions to the seasonal CO_2 cycle from various sources for the simulated point to the southwest of Baring Head. These curves were obtained by fitting the CarbonTracker/TM3 model output for the period 2003–2009 with 2-harmonic seasonal cycles. The Northern and Southern Hemisphere terrestrial influences both have peaks in late austral winter and troughs in late austral summer. The Southern Hemisphere ocean contribution has a peak in austral autumn and trough in austral spring, comparable in magnitude and leading by around 5 months the Northern and Southern Hemisphere terrestrial influences, and reflecting thermal forcing at lower latitudes rather than biological forcing at high latitudes (Takahashi et al., 2009; Heimann et al., 1998). The combination of these out-of-phase influences leads to a Baring Head peak in atmospheric CO_2 in austral winter and trough in austral summer, with comparable magnitude and phasing to the observations.

Both the oceanic and terrestrial contributions to the atmospheric CO_2 seasonal cycle are advanced in phase at Baring Head relative to the South Pole (not shown), which reflects the mixing time needed for signals to propagate from further north and explains the resulting phase difference between these two stations. The modelled Southern Ocean contribution is larger in amplitude at Baring Head than at South Pole. In the real atmosphere, this may result in a greater cancellation of the out-of-phase terrestrial contribution, potentially explaining why the observed overall amplitude is lower at Baring Head than the South Pole. However, our model simulations produce greater seasonal amplitude at Baring Head than both observed and modelled for South Pole. This highlights the sensitivity of the seasonal cycle at Baring Head to subtle shifts in timing and magnitude of the contributing influences, and suggests that seasonal CO_2 cycles in the Southern Hemisphere might be useful as a test of modelled interhemispheric transport.

Because the resulting seasonal cycle is a delicate balance between multiple processes, it varies considerably from year to year, and can be hard to detect in some years (Fig. 3). Figure 7 shows the interannually varying 5-yr-smoothed seasonal

BGD
9, 15237–15277, 2012

components from STL fits to both Baring Head and South Pole, and their similarity indicates that these variations are often consistent over large areas of the high southern latitudes. Any long-term changes in seasonal amplitude or phase at Baring Head might provide clues to trends in seasonal exchange processes. Because so much of the seasonal forcing at Baring Head comes from further to the north, these changes cannot be uniquely attributed to changes at high southern latitudes. However, by differencing the seasonal variations at Baring Head and South Pole, it might be possible to isolate the influence of Southern Hemisphere ocean fluxes, as changes in northern fluxes or interhemispheric exchange times are likely to affect both stations similarly. Figure 8 shows differences between monthly means from the Baring Head steady period record and South Pole. Also shown are linear trend lines fit to early summer and early winter months, when the modelled influence of Southern Ocean fluxes at Baring Head is maximized. Based on hypothesized changes in the upwelling-driven outgassing of CO_2 in the Southern Ocean, we might expect to see different trends in the BHD-SPO gradient in different seasons. There are no apparent differences in the summer and winter trends shown in Fig. 8, suggesting that any changes in the seasonal aspects of Southern Ocean CO_2 change are too small to be detected by this metric.

3.4 Interannual variations

The global carbon cycle and atmospheric CO_2 mole fractions vary considerably on interannual time scales (Figs. 4 and 9). Bacastow (1976) first recognized the El Niño/Southern Oscillation (ENSO) as a dominant forcing of these changes, and numerous studies have since refined our understanding of the mechanisms involved (Keeling et al., 1989a; Jones et al., 2001; Reichenau and Esser, 2003; Hashimoto et al., 2004; Zeng et al., 2005; Page et al., 2002). Positive ENSO conditions are associated with warmer and drier conditions on land, leading to decreased photosynthesis and increased respiration and fire activity, while a smaller ocean response in the opposite direction results from less outgassing of CO_2 from upwelled waters in the tropical Pacific (Feeley et al., 1999; Zeng et al., 2005). The net result for atmospheric CO_2 mole fractions is a positive correlation between CO_2 growth rate and ENSO, with CO_2 growth rate lagging ENSO by around 5 months. Terrestrial carbon exchange also responds on similar timescales to large-scale temperature fluctuations not directly related to ENSO (Keeling et al., 2001).

As Fig. 9 shows, the interannual fluctuations in CO_2 growth rate at Baring Head are very similar to those at Mauna Loa, and both are closely related to the ENSO cycle. The high CO_2 growth rates in the Baring Head record in 1973, 1979, 1983, 1987, 1998, 2002, and 2010 are all associated with leading El Niño events. The overall similarity to Mauna Loa highlights the global reach of the atmospheric CO_2 variations in response to ENSO. ENSO can explain 23 % of the variability in the interannual component of the Mauna Loa STL fit at an optimal lag of 4 months, and can explain 16 % of the variability in the interannual component of the Baring Head STL fit at an optimal lag of 6 months. The peak in Mauna Loa growth rate in 1994–95 is an example of warm global temperatures not associated with El Niño (Keeling et al., 2001), though it is only partially matched by a Baring Head excursion in 1995.

Another important interannual forcing agent is the occurrence of large volcanic eruptions, which have been shown to lead to global cooling and less respiration, as well as increased photosynthesis from more diffuse radiation as a result of aerosol scattering (Gu et al., 2003; Reichenau and Esser, 2003). These volcanic effects tend to mask or interrupt the otherwise tight connection to ENSO. For example, the extended weak El Niño that started in 1991 did not lead to positive CO_2 growth rate anomalies because of the counteracting effects of the Pinatubo eruption in June 1991 (Gu et al., 2003; Reichenau and Esser, 2003).

Interannual differences between Baring Head and Mauna Loa could result from unique ENSO forcing at high southern latitudes, different mole fraction responses in the Northern Hemisphere, or unrelated phenomena. Previous studies (Le Quéré et al., 2003; Verdy et al., 2007) have found evidence that the influence of ENSO events can propagate into the Southern Ocean and lead to stronger westerlies, greater entrainment of deep water, and anomalous carbon outgassing. The extent to which ENSO

BGD

9, 15237–15277, 2012

influences the Southern Ocean varies and this could explain some of the differences seen between Baring Head and Mauna Loa in Fig. 9. However, the 1986–1987 El Niño had less influence on the Southern Ocean (Le Quéré et al., 2003), while the Baring Head record appears to respond similarly to Mauna Loa in this event. An additional consideration in the case of Baring Head is that El Niño influences on local wind patterns could affect the number or character of steady periods selected by the data filter (Mullan, 1996).

Another important source of interannual variability at high southern latitudes is the occurrence of large-scale wind changes associated with the Southern Annular Mode (Hall and Visbeck, 2002). Positive phases of SAM are associated with increased westerlies in the Antarctic frontal zone, increased northward Ekman flow, and increased upwelling of CO_2-rich water around Antarctica. Ocean biogeochemistry models (Lenton and Matear, 2007; Lovenduski et al., 2007) and atmospheric inverse models (Butler et al., 2007) suggest anomalous Southern Ocean CO_2 outgassing of around 0.1 $\mathrm{Pg\,C\,yr^{-1}}$ per standard deviation of SAM. Butler et al. (2007) was able to identify signals in atmospheric CO_2 potentially associated with these flux changes by correlating month-to-month tendencies in CO_2 to the SAM index. The correlations were greatest at Palmer Station Antarctica (PSA) and decreased further from the high-latitude Southern Ocean. We have repeated the Butler et al. (2007) analysis on our Baring Head data and found no significant correlation. This could either be because the postulated high-latitude Southern Ocean flux changes have a greater impact at PSA than they do at Baring Head, or, as discussed by Bulter et al. (2007), the correlation at PSA could result from local changes in wind direction that are different at Baring Head. The significant decrease in long-term growth rate (Fig. 3) and increase in seasonal amplitude (Fig. 7) from 1991–1994 in the Baring Head record could be associated with the Pinatubo eruption as discussed above, but could also be related to a large negative excursion in SAM that occurred at the same time. Further research on possible mechanisms driving these CO_2 changes is warranted.

Figure 10 shows the difference between the interannual and trend components of the Baring Head and Mauna Loa STL fits, while Fig. 11 shows the difference between the interannual and trend components of the Baring Head and South Pole STL fits. Overall levels of interannual variability for high-latitude Southern Ocean carbon fluxes based on observational and modelling studies are on the order of ±0.15 $\mathrm{Pg\,C\,yr^{-1}}$ (1 sigma) (Butler et al., 2007; Lenton and Matear, 2007; Lovenduski et al., 2007; Louanchi and Hoppeman, 2000; Le Quéré et al., 2003). Based on our TM3 sensitivities, we would expect this to appear in the BHD-MLO difference at the ±0.2 ppm level and the BHD-SPO difference at the ±0.05 ppm level. From Figs. 10 and 11, it is apparent that other processes such as lower latitude Southern Ocean fluxes, Northern Hemisphere processes combined with interhemispheric transport variability, or measurement or data-filtering biases must lead to the larger interannual variations of ±0.3 to 0.5 ppm.

3.5 Long-term trends

Despite the fact that year-to-year variations in Southern Ocean CO_2 fluxes have relatively small impacts on year-to-year atmospheric CO_2 gradients, long-term trends in Southern Ocean carbon exchange can have major impacts on future global atmospheric CO_2 mole fractions. Because of the large exchanges of heat and gases that occur between the atmosphere and deep ocean waters at high southern latitudes, carbon fluxes in the Southern Ocean have long been recognized as a dominant factor in determining the ocean's uptake of anthropogenic CO_2 (Knox and McElroy, 1984; Siegenthaler and Wenk, 1984; Sarmiento and Toggweiler, 1984; Sarmiento et al., 1998; Caldeira and Duffy, 2000). CO_2 fluxes in this region are currently a sensitive balance between opposing thermal and biologic forcing (Sarmiento et al., 1998), and their response to climate change is likely to be a complex combination of dynamic effects on opposing natural and anthropogenic fluxes (Le Quéré et al., 2007; Lenton and Matear, 2007; Lovenduski et al., 2007; Zickfeld et al., 2008, Lenton et al., 2009; Lovenduski and Ito, 2009). Uncertainties in the future behaviour of the global ocean carbon cycle as a whole lead to predictions with a range of 4 $\mathrm{Pg\,C\,yr^{-1}}$ in 2050 (Friedlingstein et al.,

BGD
9, 15237–15277, 2012

2006), with a large contribution to this range presumably coming from the Southern Ocean (Friedlingstein et al., 2006; Sarmiento et al., 1998; Caldeira and Duffy, 2000; Le Quéré et al., 2007; Zickfeld et al., 2008, Lenton et al., 2009; Lovenduski and Ito, 2009).

For these reasons, much effort has recently gone into investigating whether and in what direction high-latitude Southern Ocean carbon exchanges are already responding to anthropogenic forcing. Evidence suggests that as a result of ozone depletion and climate change, Antarctic circumpolar winds have increased over the past several decades and will continue to increase in the future (Thompson and Solomon, 2002; Marshall, 2003). While it is still unclear what effect these changes are having on deep-water ventilation (Saenko et al., 2005; Böning et al., 2008), it is also unclear what effect potential changes in ventilation would have on carbon cycling (Le Quéré et al., 2007; Lenton and Matear, 2007; Lovenduski et al., 2007; Zickfeld et al., 2008; Lenton et al., 2009; Lovenduski and Ito, 2009; Takahashi et al., 2009). Le Quéré et al. (2007) suggested that the ongoing wind changes have increased the upwelling of carbon-rich deep waters and the outgassing of natural CO_2 from the Southern Ocean. They presented evidence from a biologic ocean model and a set of atmospheric inversions that the rate of increase in Southern Ocean carbon uptake has slowed over the past decade, resulting in a smaller uptake in proportion to the increasing atmospheric burden. This result is consistent with long-term trends in high-latitude Southern Ocean $p\mathrm{CO_2}$ data (Takahashi et al., 2009; Metzl, 2009) showing a faster CO_2 increase in surface waters than the atmosphere. However, the result remains controversial. Law et al. (2008) argued that the stations available for the atmospheric inversion were too few to obtain robust trends, and Zickfeld et al. (2009) showed results from a different ocean model that indicated increased overturning has led to greater uptake of anthropogenic carbon in the Southern Ocean, associated with the sinking of northward flowing surface waters.

An hourly mean version of the Baring Head record was used along with analyzed winds in the atmospheric inversion of Le Quéré et al. (2007), so we are not in a position to independently assess their result. However, it is useful to investigate what aspects of

BGD
9, 15237–15277, 2012

A 39-yr atmospheric CO_2 record from Baring Head, New Zealand

B. B. Stephens et al.

the atmospheric data may be driving the inverse result and ask how large the expected trend signals are with respect to natural variability, and how robust the attribution of trends is with respect to other natural influences and potential measurement biases. The long-term trend in the BHD-SPO difference, shown in Fig. 11, is fairly constant for the 1978–2000 period, but there is a suggestion of a slight increase at Baring Head relative to South Pole of around 0.3 ppm over the last 10 yr of the record.

The expected changes in atmospheric CO_2 gradients from the Le Quéré et al. (2007) study are quite small. Scaling the 0.2 $\mathrm{Pg\,C\,yr^{-1}}$ expected increase in uptake over the 1968–2005 period by the TM3 sensitivities only gives a −0.09 ppm expected shift in the atmospheric BHD-SPO gradient over this period. Furthermore, the proposed levelling off in this trend and decreasing efficiency of anthropogenic uptake, by about 0.1 $\mathrm{Pg\,C\,yr^{-1}}$ from 1985–2005, amounts to a BHD-SPO signal of only +0.04 ppm over 20 yr. This estimate is in general agreement with the actual combination of ocean and atmosphere models used by Le Quéré et al. (2007), which produce a change between Macquarie Island (MQA, 54°30′ S, 158°57′ E) and South Pole associated with the reduced deep-water upwelling of +0.05 ppm from 1985–2005. This number was obtained by comparing model time series (C. Rödenbeck, personal communication, 2010) for Macquarie Island and South Pole for both the constant and observed wind simulations. We used model output at Macquarie Island instead of Baring Head because the output is not selected for steady-CO_2 southerly wind conditions. Such small changes over 20 yr are unlikely to be detectable in comparing any two individual atmospheric CO_2 records. The suggestion in the observations of a +0.3 ppm change since 2001 could reflect an even larger change in Southern Ocean fluxes than modelled by Le Quéré et al. (2007), but this change is not statistically robust with respect to potential measurement biases of up to 0.3 ppm (Brailsford et al., 2012).

More generally, the trends in the BHD-MLO differences in Fig. 10 are consistent with increasing fossil-fuel emissions in the Northern Hemisphere and increasing uptake of anthropogenic CO_2 in the low and high latitude Southern Ocean in response to those emissions. Notably, the rate of increase in this difference does not appear to

BGD
9, 15237–15277, 2012

slow since 2000. The expected change associated with increases in fossil-fuel emissions over the 39-yr record (Boden et al., 2009), obtained by scaling the TM3 sensitivities discussed above, is a −2.8 ppm change in the BHD-MLO difference, which would be reduced in magnitude by increased northern terrestrial sinks but made more negative by increased Southern Ocean sinks over the same period. For BHD-MLO, scaling the ocean fluxes modelled by Le Quéré et al. (2007) by our TM3 results, suggests a −0.25 ppm change due to a long-term 0.2 $\mathrm{Pg\,C\,yr^{-1}}$ increase in Southern Ocean CO_2 uptake, and a +0.13 ppm change associated with the proposed levelling off of the uptake trend from 1985–2005. Again, the actual combination of ocean and atmosphere models used by Le Quéré et al. (2007) agrees with this scaling, giving a change of +0.11 ppm for MQA-MLO from 1985–2005 (Christian Rödenbeck, personal communication, 2010). The expected change in BHD-MLO associated with the Southern Ocean is larger than that for BHD-SPO, but again is small with respect to natural variability, and with respect to compatibility estimates for the measurements.

In practical terms, given the number of stations used, the complexity of atmospheric transport, and the complex nature of the inversion process, it can be very difficult to determine exactly what drives a particular atmospheric inversion result (Gurney et al., 2004; Rödenbeck et al., 2003; Stephens et al., 2007). More work is needed in connection with atmospheric inverse models to trace results to quantitative features of the data so that they can be assessed in terms of potential data biases (Law et al., 2008). In addition, given that potential systematic biases between individual CO_2 station records and different CO_2 measuring labs is still significant (WMO, 2011), sensitivity studies should be conducted in which mole fractions at individual stations are offset by several tenths of ppm over various time periods to assess the robustness of the inversion results (Rödenbeck et al., 2006; Law et al., 2008; Masarie et al., 2011).

BGD
9, 15237–15277, 2012

4 Conclusions

We have presented an analysis of a newly reprocessed version of the 39-yr continuous atmospheric CO_2 record from Baring Head, New Zealand. This record is the longest in situ CO_2 measurement record in the Southern Hemisphere, and second longest globally, and has applicability in a wide range of carbon cycle studies. Consistent with original goals, Baring Head has proved to be a good location for observing clean marine boundary-layer air arriving from the high-latitude Southern Ocean that has been isolated from contact with land for extended periods of time. Depending on air-mass history, atmospheric CO_2 at Baring Head responds to processes on local to global scales, and one of the advantages of a continuous record is that we can carefully filter the data for clean background air conditions (Fig. 3).

We have used the filtered steady period time series for comparisons to the background stations South Pole and Mauna Loa from the SIO network, and to atmospheric model simulations. These comparisons reveal a seasonal cycle that results from a combination of Northern and Southern Hemisphere land and ocean influences and is sensitive to interhemispheric transport. Interannual variations in atmospheric CO_2 growth rate at Baring Head are strongly correlated with ENSO, reflecting tropical and possibly Southern Ocean carbon cycle responses. The multi-decadal trends at Baring Head follow those at South Pole closely throughout the record, with a suggestion of a possible divergence by $+0.3\,\mathrm{ppm\,decade^{-1}}$ since 2001. The differences with respect to Mauna Loa grow steadily in response to increasing emissions in the Northern Hemisphere, and do not appear to be levelling off.

To date, the impact of the proposed $0.1\,\mathrm{Pg\,C\,yr^{-1}\,decade^{-1}}$ flux changes on atmospheric gradients are below detection limits, given uncertainties in comparing CO_2 records from independent stations and laboratories and the limited number of atmospheric CO_2 stations in the Southern Hemisphere. Our ability to detect and monitor changes in Southern Ocean carbon fluxes would be advanced by improved compatibility between sites and laboratories to the 0.05 ppm level long recommended by WMO

BGD
9, 15237–15277, 2012

(WMO, 2011) and by a significantly expanded observing network. At present, this ability is critically dependent on the continuation of the few existing long time series of atmospheric CO_2, such as that from Baring Head. Aspects of this record, including (1) the seasonal cycle, (2) interannual variations in the seasonal cycle, (3) the growth-rate relationship with ENSO, (4) the non-ENSO related interannual variability, (5) the long-term trends with respect to South Pole and Mauna Loa, and (6) changes in these long-term trends, can provide important data-based tests of coupled atmosphere-ocean models and their ability to accurately represent the effect of climate change on Southern Ocean carbon cycling. We encourage the continued use of the Baring Head atmospheric CO_2 record in such efforts.

Acknowledgements. We would like to thank the many people who have helped to maintain the Baring Head CO_2 measurements over the past 4 decades, in particular Dave Keeling, Dave Lowe, Peter Guenther, Athol Rafter, Owen Rowse, Peter Pohl, Ross Martin, Rowena Moss, Bruce Speding, Ian Hemmingsen, and Ed Hutchinson. Mike Harvey has also helped support the instrumentation and provided valuable comments on the manuscript. We gratefully acknowledge Ralph Keeling for providing SIO flask data from Mauna Loa and South Pole for use in this study. We would also like to thank Christian Rödenbeck for providing model output. CarbonTracker 2010 results were provided by NOAA ESRL, Boulder, Colorado, USA from the website at http://carbontracker.noaa.gov. We thank Maritime Safety NZ and Greater Wellington Regional Council for assistance and site access. NIWA research is core funded through the Ministry of Business, Innovation and Employment. NCAR is sponsored by the National Science Foundation.

References

Bacastow, R. B.: Modulation of atmospheric carbon-dioxide by the Southern Oscillation, Nature, 261, 116–118, doi:10.1038/261116a0, 1976.

Baker, D. F., Law, R. M., Gurney, K. R., Rayner, P., Peylin, P., Denning, A. S., Bousquet, P., Bruhwiler, L., Chen, Y.-H., Ciais, P., Fung, I. Y., Heimann, M., John, J., Maki, T., Maksyutov, S., Masarie, K., Prather, M., Pak, B., Taguchi, S., and Zhu, Z.: TransCom 3 inversion intercomparison: impact of transport model errors on the interannual variability of regional

CO_2 fluxes, 1988–2003, Global Biogeochem. Cy., 20, GB1002, doi:10.1029/2004GB002439, 2006.
Boden, T. A., Marland, G., and Andres, R. J.: Global, Regional, and National Fossil-Fuel CO_2 Emissions, Carbon Dioxide Information Analysis Center, Oak Ridge National Laboratory, US Department of Energy, Oak Ridge, Tenn., USA, doi:10.3334/CDIAC/00001, 2009.
Böning, C. W., Dispert, A., Visbeck, M., Rintoul, S. R., and Schwarzkopf, F. U.: The response of the Antarctic Circumpolar Current to recent climate change, Nat. Geosci., 1, 864–869, doi:10.1038/ngeo362, 2008.
Brailsford, G. W., Stephens, B. B., Gomez, A. J., Riedel, K., Mikaloff Fletcher, S. E., Nichol, S. E., and Manning, M. R.: Long-term continuous atmospheric CO_2 measurements at Baring Head, New Zealand, Atmos. Meas. Tech. Discuss., 5, 5889–5912, doi:10.5194/amtd-5-5889-2012, 2012.
Butler, A. H., Thompson, D. W. J., and Gurney, K. R.: Observed relationships between the southern annular mode and atmospheric carbon dioxide, Global Biogeochem. Cy., 21, GB4014, doi:10.1029/2006GB002796, 2007.
Caldeira, K. and Duffy, P. B.: The role of the Southern Ocean in uptake and storage of anthropogenic carbon dioxide, Science, 287, 620–622, doi:10.1126/science.287.5453.620, 2000.
Cleveland, R. B., Cleveland, W. S., McRae, J. E., and Terpenning, I.: STL: A seasonal-trend decomposition procedure based on loess, J. Off. Stat., 6, 3–73, 1990.
Cleveland, W. S. and McRae, J. E.: The use of loess and STL in the analysis of atmospheric CO_2 and related data, in: The Statistical Treatment of CO_2 Data Records, edited by: Elliot, W. P., National Oceanic and Atmospheric Administration, Silver Springs, Maryland, 61–81, 1989.
Dargaville, R. J., Heimann, M., McGuire, A. D., Prentice, I. C., Kicklighter, D. W., Joos, F., Clein, J. S., Esser, G., Foley, J., Kaplan, J., Meier, R. A., Melillo, J. M., Moore, B., Ramankuty, N., Reichenau, T., Schloss, A., Sitch, S., Tian, H., Williams, L. J., and Wittenberg, U.: Evaluation of terrestrial carbon cycle models with atmospheric CO_2 measurements: results from transient simulations considering increasing CO_2, climate, and land-use effects, Global Biogeochem. Cy., 16, 1092, doi:10.1029/2001GB001426, 2002.
Dargaville, R. J., Doney, S. C., and Fung, I. Y.: Inter-annual variability in the interhemispheric atmospheric CO_2 gradient: contributions from transport and the seasonal rectifier, Tellus B, 55, 711–722, 2003.

BGD
9, 15237–15277, 2012

A 39-yr atmospheric CO_2 record from Baring Head, New Zealand

B. B. Stephens et al.

Erickson, D. J., Rasch, P. J., Tans, P. P., Friedlingstein, P., Ciais, P., Maier-Reimer, E., Six, K., Fischer, C. A., and Walters, S.: The seasonal cycle of atmospheric CO_2: a study based on the NCAR Community Climate Model (CCM2), J. Geophys. Res., 101, 15079–15097, doi:10.1029/95JD03680, 1996.

Friedlingstein, P., Cox, P., Betts, R., Bopp, L., Von Bloh, W., Brovkin, V., Cadule, P., Doney, S., Eby, M., Fung, I., Bala, G., John, J., Jones, C., Joos, F., Kato, T., Kawamiya, M., Knorr, W., Lindsay, K., Matthews, H. D., Raddatz, T., Rayner, P., Reick, C., Roeckner, E., Schnitzler, K.-G., Schnur, R., Strassmann, K., Weaver, A. J., Yoshikawa, C., and Zeng, N.: Climate-carbon cycle feedback analysis: results from the C^4MIP model intercomparison, J. Climate, 19, 3337–3353, doi:.org/10.1175/JCLI3800.1, 2006.

Globalview-CO_2: Cooperative Atmospheric Data Integration Project – Carbon Dioxide, CD-ROM, NOAA ESRL, Boulder, Colorado, also available at: ftp://ftp.cmdl.noaa.gov, Path: ccg/co2/GLOBALVIEW, 2011.

Gordon, N. D.: Computer-derived air trajectories, Scientific Report 22, New Zealand Meteorological Service, Wellington, New Zealand, 1–13, 1986.

Gruber, N., Gloor, M., Fletcher, S. E. M., Doney, S. C., Dutkiewicz, S., Follows, M. J., Gerber, M., Jacobson, A. R., Joos, F., Lindsay, K., Menemenlis, D., Mouchet, A., Mueller, S. A., Sarmiento, J. L., and Takahashi, T.: Oceanic sources, sinks, and transport of atmospheric CO_2, Global Biogeochem. Cy., 23, GB1005, doi:10.1029/2008GB003349, 2009.

Gu, L., Baldocchi, D., Verma, S. B., Black, T. A., Vesala, T., Falge, E. M., and Dowty, P. R.: Advantages of diffuse radiation for terrestrial ecosystem productivity, J. Geophys. Res., 107, 4050, doi:10.1029/2001JD001242, 2002.

Gurney, K. R., Law, R. M., Denning, A. S., Rayner, P. J., Baker, D., Bousquet, P., Bruhwiler, L., Chen, Yu-Han, Ciais, P., Fan, S., Fung, I. Y., Gloor, M., Heimann, M., Higuchi, K., John, J., Maki, T., Maksyutov, S., Masarie, K., Peylin, P., Prather, M., Pak, B. C., Randerson, J., Sarmiento, J., Taguchi, S., Takahashi, T., and Yuen, C.-W.: Towards robust regional estimates of CO_2 sources and sinks using atmospheric transport models, Nature, 415, 626–630, doi:10.1038/415626a, 2002.

Gurney, K. R., Law, R. M., Denning, A. S., Rayner, P. J., Baker, D., Bousquet, P., Bruhwiler, L., Chen, Yu-Han, Ciais, P., Fan, S., Fung, I. Y., Gloor, M., Heimann, M., Higuchi, K., John, J., Kowalczyk, E., Maki, T., Maksyutov, S., Peylin, P., Prather, M., Pak, B. C., Sarmiento, J., Taguchi, S.: Transcom 3 CO_2 inversion intercomparison: 1. annual mean control results and sensitivity to transport and prior flux information, Tellus B, 55, 555–579, doi:10.1034/j.1600-0889.2003.00049.x, 2003.

Gurney, K. R., Law, R. M., Denning, A. S., Rayner, P. J., Pak, B. C., Baker, D., Bousquet, P., Bruhwiler, L., Chen, Y.-H., Ciais, P., Fung, I. Y., Heimann, M., John, J., Maki, T., Maksyutov, S., Peylin, P., Prather, M., and Taguchi, S.: Transcom 3 inversion intercomparison: model mean results for the estimation of seasonal carbon sources and sinks, Global Biogeochem. Cy., 18, GB1010, doi:10.1029/2003GB002111, 2004.

Gurney, K. R., Baker, D., Rayner, P., and Denning, S.: Interannual variations in continental-scale net carbon exchange and sensitivity to observing networks estimated from atmospheric CO_2 inversions for the period 1980 to 2005, Global Biogeochem. Cy., 22, GB3025, doi:10.1029/2007GB003082, 2008.

Hall, A. and Visbeck, M.: Synchronous variability in the Southern Hemisphere atmosphere, sea ice, and ocean resulting from the annular mode, J. Climate, 15, 3043–3057, 2002.

Hashimoto, H., Nemani, R., White, M., Jolly, W., Piper, S., Keeling, C., Myneni, R., and Running, S.: El Niño-Southern Oscillation-induced variability in terrestrial carbon cycling, J. Geophys. Res.-Atmos., 109, D23110, doi:10.1029/2004JD004959, 2004.

Heimann, M. and Keeling, C. D.: A three-dimensional model of atmospheric CO_2 transport based on observed winds: 2. model description and simulated tracer experiments, in: Geophysical Monograph 55, Aspects of climate variability in the Pacific and the Western Americas, edited by: Peterson, D. H., American Geophysical Union, Washington, DC, 237–275, 1989.

Heimann, M. and Körner, S.: The global atmospheric tracer model TM3, in: Technical Report, vol. 5, edited by: Max-Planck-Institut für Biogeochemie, Max-Planck-Institut für Biogeochemie, Jena, Germany, 131 pp., 2003.

Heimann, M., Esser, G., Haxeltine, A., Kaduk, J., Kicklighter, D. W., Knorr, W., Kohlmaier, G. H., McGuire, A. D., Melillo, J., Moore, B., Otto, R. D., Prentice, I. C., Sauf, W., Schloss, A., Sitch, S., Wittenberg, U., and Wurth, G.: Evaluation of terrestrial Carbon Cycle models through simulations of the seasonal cycle of atmospheric CO_2: first results of a model intercomparison study, Global Biogeochem. Cy., 12, 1–24, 1998.

IPCC: Contribution of Working Group I to the Fourth Assessment Report of the Intergovernmental Panel on Climate Change, Cambridge University Press, Cambridge, UK and New York, NY, USA, 2007.

Jones, C., Collins, M., Cox, P., and Spall, S.: The carbon cycle response to ENSO: a coupled climate-carbon cycle model study, J. Climate, 14, 4113–4129, 2001.
Kawa, S., Erickson, D., Pawson, S., and Zhu, Z.: Global CO_2 transport simulations using meteorological data from the NASA data assimilation system, J. Geophys. Res.-Atmos., 109, D18312, doi:10.1029/2004JD004554, 2004.
Keeling, C. D.: The concentration and isotopic abundances of carbon dioxide in rural and marine air, Geochim. Cosmochim. Ac., 24, 277–298, 1961.
Keeling, C. D., Bacastow, R. B., Carter, A. F., Piper, S. C., Whorf, T. P., Heimann, M., Mook, W. G., and Roeloffzen, H.: A three dimensional model of atmospheric CO_2 transport based on observed winds: 1. analysis of observational data, in: Geophysical Monograph 55, Aspects of Climate Variability in the Pacific and the Western Americas, edited by: Peterson, D. H., American Geophysical Union, Washington, DC, 165–236, 1989a.
Keeling, C. D., Piper, S. C., and Heimann, M.: A three-dimensional model of atmospheric CO_2 transport based on observed winds: 4. Mean annual gradients and interannual variations, in: Geophysical Monograph 55, Aspects of Climate Variability in the Pacific and the Western Americas, edited by: Peterson, D. H., American Geophysical Union, Washington, DC, 305–363, 1989b.
Keeling, C. D., Piper, S. C., Bacastow, R. B., Wahlen, M., Whorf, T. P., Heimann, M., and Meijer, H. A.: Exchanges of atmospheric CO_2 and $^{13}CO_2$ with the terrestrial biosphere and oceans from 1978 to 2000. I. Global aspects, Scripps Institution of Oceanography, San Diego, 2001.
Kidson, J.: An analysis of New Zealand synoptic types and their use in defining weather regimes, Int. J. Climatol., 20, 299–316, 2000.
Knox, F. and McElroy, M. B.: Changes in atmospheric CO_2: influence of the marine biota at high latitude, J. Geophys. Res., 89, 4629–4637, 1984.
Law, R. M. Chen, Y.-H., Gurney, K. R., and Transcom 3 modellers: Transcom 3 CO_2 Inversion Intercomparison: 2. sensitivity of annual mean results to data choices, Tellus B, 55, 580–595, doi:10.1034/j.1600-0889.2003.00053.x, 2003.
Law, R. M., Matear, R. J., and Francey, R. J.: Comment on “Saturation of the Southern Ocean CO_2 sink due to recent climate change”, Science, 319, 570, doi:10.1126/science.1149077, 2008.
Le Quéré, C., Aumont, O., Bopp, L., Bousquet, P., Ciais, P., Francey, R., Heimann, M., Keeling, C. D., Keeling, R. F., Kheshgi, H., Peylin, P., Piper, S. C., Prentice, I. C., and Rayner, P. J.:

BGD
9, 15237–15277, 2012

A 39-yr atmospheric CO_2 record from Baring Head, New Zealand

B. B. Stephens et al.

Two decades of ocean CO_2 sink and variability, Tellus B, 55, 649–656, doi:10.1034/j.1600-0889.2003.00043.x, 2003.

Le Quéré, C., Rödenbeck, C., Buitenhuis, E. T., Conway, T. J., Langenfelds, R., Gomez, A., Labuschagne, C., Ramonet, M., Nakazawa, T., Metzl, N., Gillett, N., and Heimann, M.: Saturation of the Southern Ocean CO_2 Sink due to recent climate change, Science, 316, 1735, doi:10.1126/science.1136188, 2007.

Lenton, A. and Matear, R. J.: Role of the Southern Annular Mode (SAM) in Southern Ocean CO_2 uptake, Global Biogeochem. Cy., 21, GB2016, doi:10.1029/2006GB002714, 2007.

Lenton, A., Codron, F., Bopp, L., Metzl, N., Cadule, P., Tagliabue, A., and Le Sommer, J.: Stratospheric ozone depletion reduces ocean carbon uptake and enhances ocean acidification, Geophys. Res. Lett., 36, L12606, doi:10.1029/2009GL038227, 2009.

Louanchi, F. and Hoppema, M.: Interannual variations of the Antarctic Ocean CO_2 uptake from 1986 to 1994, Mar. Chem., 72, 103–114, 2000.

Lovenduski, N. S. and Ito, T.: The future evolution of the Southern Ocean CO_2 sink, J. Mar. Res., 67, 597–617, 2009.

Lovenduski, N. S., Gruber, N., Doney, S. C., and Lima, I. D.: Enhanced CO_2 outgassing in the Southern Ocean from a positive phase of the Southern Annular Mode, Global Biogeochem. Cy., 21, GB2026, doi:10.1029/2006GB002900, 2007.

Lowe, D. C., Guenther, P. R., and Keeling, C. D.: The concentration of atmospheric carbon dioxide at Baring Head, New Zealand, Tellus, 31, 58–67, 1979.

Manning, M. R. and Pohl, K. P.: Atmospheric carbon dioxide monitoring in New Zealand, 1971–1985, DSIR, Institute of Nuclear Sciences, Lower Hutt, New Zealand, available at: http://webcat.niwa.co.nz/documents/INS-R-350.pdf, last access: August 2012, 1986.

Manning, M. R., Gomez, A. J., and Pohl, K. P.: Atmospheric CO_2 record from in situ measurements at Baring Head, in: Trends '93: a Compendium of Data on Global Change, ORNL/CDIAC-65, edited by: Boden, T. A., Kaiser, D. P., Sepanski, R. J., and Stoss, F. W., Oak Ridge, TN, USA, 1994.

Marshall, G.: Trends in the southern annular mode from observations and reanalyses, J. Climate, 16, 4134–4143, 2003.

Masarie, K. A., Petron, G., Andrews, A., Bruhwiler, L., Conway, T. J., Jacobson, A. R., Miller, J. B., Tans, P. P., Worthy, D. E., and Peters, W.: Impact of CO_2 measurement bias on CarbonTracker surface flux estimates, J. Geophys. Res.-Atmos., 116, D17305, doi:10.1029/2011JD016270, 2011.

Metzl, N.: Decadal increase of oceanic carbon dioxide in Southern Indian Ocean surface waters (1991–2007), Deep-Sea Res. Pt. II, 56, 607–619, 2009.

Mullan, B.: Effects of ENSO on New Zealand and the South Pacific, in: Prospects and Needs for Climate Forecasting, Miscellaneous Series 34, edited by: Braddock, D., Royal Society of New Zealand, Wellington, New Zealand, 23–27, 1996.

Nevison, C. D., Mahowald, N. M., Doney, S. C., Lima, I. D., Van der Werf, G. R., Randerson, J. T., Baker, D. F., Kasibhatla, P., and McKinley, G. A.: Contribution of ocean, fossil fuel, land biosphere, and biomass burning carbon fluxes to seasonal and interannual variability in atmospheric CO_2, J. Geophys. Res., 113, G01010, doi:10.1029/2007JG000408, 2008.

Page, S., Siegert, F., Rieley, J., Boehm, H., Jaya, A., and Limin, S.: The amount of carbon released from peat and forest fires in Indonesia during 1997, Nature, 420, 61–65, 2002.

Patra, P. K., Law, R. M., Peters, W., Rödenbeck, C., Takigawa, M., Aulagnier, C., Baker, I., Bergmann, D. J., Bousquet, P., Brandt, J., Bruhwiler, L., Cameron-Smith, P. J., Christensen, J. H., Delage, F., Denning, A. S., Fan, S., Geels, C., Houweling, S., Imasu, R., Karstens, U., Kawa, S. R., Kleist, J., Krol, M. C., Lin, S.-J., Lokupitiya, R., Maki, T., Maksyutov, S., Niwa, Y., Onishi, R., Parazoo, N., Pieterse, G., Rivier, L., Satoh, M., Serrar, S., Taguchi, S., Vautard, R., Vermeulen, A. T., and Zhu, Z.: TransCom model simulations of hourly atmospheric CO_2: analysis of synoptic-scale variations for the period 2002–2003, Global Biogeochem. Cy., 22, GB4013, doi:10.1029/2007GB003081, 2008.

Pearman, G. I. and Hyson, P.: Activities of the global biosphere as reflected in atmospheric CO_2 records, J. Geophys. Res., 85, 4457–4467, 1980.

Peters, W., Jacobson, A. R., Sweeney, C., Andrews, A. E., Conway, T. J., Masarie, K., Miller, J. B., Bruhwiler, L. M. P., Petron, G., Hirsch, A. I., Worthy, D. E. J., van der Werf, G. R., Randerson, J. T., Wennberg, P. O., Krol, M. C., and Tans, P. P.: An atmospheric perspective on North American carbon dioxide exchange: CarbonTracker, P. Natl. Acad. Sci. USA, 104, 18925–18930, 2007.

Reichenau, T. and Esser, G.: Is interannual fluctuation of atmospheric CO_2 dominated by combined effects of ENSO and volcanic aerosols?, Global Biogeochem. Cy., 17, 1094, doi:10.1029/2002GB002025, 2003.

Rödenbeck, C., Houweling, S., Gloor, M., and Heimann, M.: CO_2 flux history 1982–2001 inferred from atmospheric data using a global inversion of atmospheric transport, Atmos. Chem. Phys., 3, 1919–1964, doi:10.5194/acp-3-1919-2003, 2003.

Rödenbeck, C., Conway, T. J., and Langenfelds, R. L.: The effect of systematic measurement errors on atmospheric CO_2 inversions: a quantitative assessment, Atmos. Chem. Phys., 6, 149–161, doi:10.5194/acp-6-149-2006, 2006.

Roy, T., Rayner, P., Matear, R., and Francey, R.: Southern Hemisphere ocean CO_2 uptake: reconciling atmospheric and oceanic estimates, Tellus B, 55, 701–710, 2003.

Saenko, O., Fyfe, J., and England, M.: On the response of the oceanic wind-driven circulation to atmospheric CO_2 increase, Clim. Dynam., 25, 415–426, 2005.

Sarmiento, J. L. and Toggweiler, J. R.: New model for the role of the oceans in determining atmospheric P_{CO_2}, Nature, 308, 621–624, 1984.

Sarmiento, J. L., Hughes, T. M. C., Stouffer, R. J., and Manabe, S.: Simulated response of the ocean carbon cycle to anthropogenic climate warming, Nature, 393, 245–249, 1998.

Siegenthaler, U. and Wenk, T.: Rapid atmospheric CO_2 variations and ocean circulation, Nature, 308, 624–626, 1984.

Stephens, B. B., Gurney, K. R., Tans, P. P., Sweeney, C., Peters, W., Bruhwiler, L., Ciais, P., Ramonet, M., Bousquet, P., Nakazawa, T., Aoki, S., Machida, T., Inoue, G., Vinnichenko, N., Lloyd, J., Jordan, A., Heimann, M., Shibistova, O., Langenfelds, R. L., Steele, L. P., Francey, R. J., and Denning, A. S.: Weak northern and strong tropical land carbon uptake from vertical profiles of atmospheric CO_2, Science, 316, 1732, doi:10.1126/science.1137004, 2007.

Takahashi, T., Sutherland, S. C., Wanninkhof, R., Sweeney, C., Feely, R. A., Chipman, D. W., Hales, B., Friederich, G., Chavez, F., Sabine, C., Watson, A., Bakker, D. C. E., Schuster, U., Metzl, N., Yoshikawa-Inoue, H., Ishii, M., Midorikawa, T., Nojiri, Y., Koertzinger, A., Steinhoff, T., Hoppema, M., Olafsson, J., Arnarson, T. S., Tilbrook, B., Johannessen, T., Olsen, A., Bellerby, R., Wong, C. S., Delille, B., Bates, N. R., and de Baar, H. J. W.: Climatological mean and decadal change in surface ocean $p$$CO_2$, and net sea-air CO_2 flux over the global oceans, Deep-Sea Res. Pt. II, 56, 554–577, 2009.

Thompson, D. W. J. and Solomon, S.: Interpretation of recent Southern Hemisphere climate change, Science, 296, 895, doi:10.1126/science.1069270, 2002.

Verdy, A., Dutkiewicz, S., Follows, M. J., Marshall, J., and Czaja, A.: Carbon dioxide and oxygen fluxes in the Southern Ocean: mechanisms of interannual variability, Global Biogeochem. Cy., 21, GB2020, doi:10.1029/2006GB002916, 2007.

Wetzel, P., Winguth, A., and Maier-Reimer, E.: Sea-to-air CO_2 flux from 1948 to 2003: a model study, Global Biogeochem. Cy., 19, GB2005, doi:10.1029/2004GB002339, 2005.

WDCGG: DVD No. 4, WMO World Data Centre for Greenhouse Gases, Tokyo, Japan, available at: http://ds.data.jma.go.jp/gmd/wdcgg/pub/products/cd-rom/dvd_04, 2012.

WMO: Report of the 15th WMO/IAEA Meeting of Experts on Carbon Dioxide, Other Greenhouse Gases and Related Tracers Measurement Techniques, edited by: Brand, W., WMO TD No. 1553, Jena, Germany, 2011.

Wolter, K. and Timlin, M. S.: Monitoring ENSO in COADS with a seasonally adjusted principal component index, in: Proc. of the 17th Climate Diagnostics Workshop, Norman, OK, NOAA/NMC/CAC, NSSL, Oklahoma Clim. Survey, CIMMS and the School of Meteor., Univ. of Oklahoma, 52–57, 1993.

Zeng, N., Mariotti, A., and Wetzel, P.: Terrestrial mechanisms of interannual CO_2 variability, Global Biogeochem. Cy., 19, GB1016, doi:10.1029/2004GB002273, 2005.

Zickfeld, K., Fyfe, J. C., Eby, M., and Weaver, A. J.: Comment on “Saturation of the Southern Ocean CO_2 Sink Due to Recent Climate Change”, Science, 319, 570, doi:10.1126/science.1146886, 2008.

BGD

9, 15237–15277, 2012

A 39-yr atmospheric CO_2 record from Baring Head, New Zealand

B. B. Stephens et al.

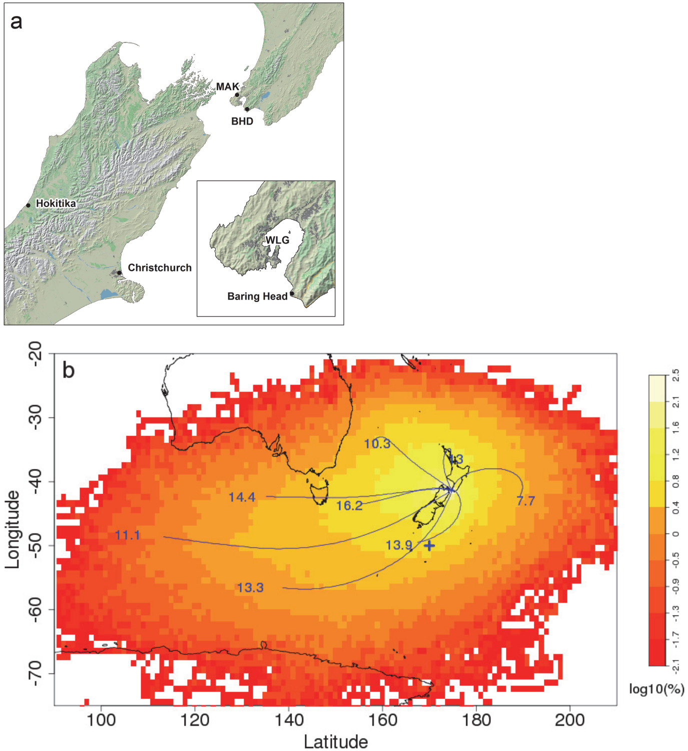

Fig. 1. Maps showing **(a)** the location of Baring Head (BHD) and other landmarks, and **(b)** clustered results of 20 yr of twice-daily 4-day back-trajectory calculations, with percentages indicated for each cluster. In **(a)**, labels also indicate Makara (MAK) and Wellington (WLG), and colors indicate forests (green), inland water (blue), populated areas (dark gray), non-forested land (beige), and above tree line (light gray). In **(b)**, colour shading indicates a logarithm of the percentage of trajectories crossing a given latitude/longitude square, and a + symbol indicates the location of TM3 model output used for comparison to steady-period data.

BGD
9, 15237–15277, 2012

A 39-yr atmospheric CO_2 record from Baring Head, New Zealand

B. B. Stephens et al.

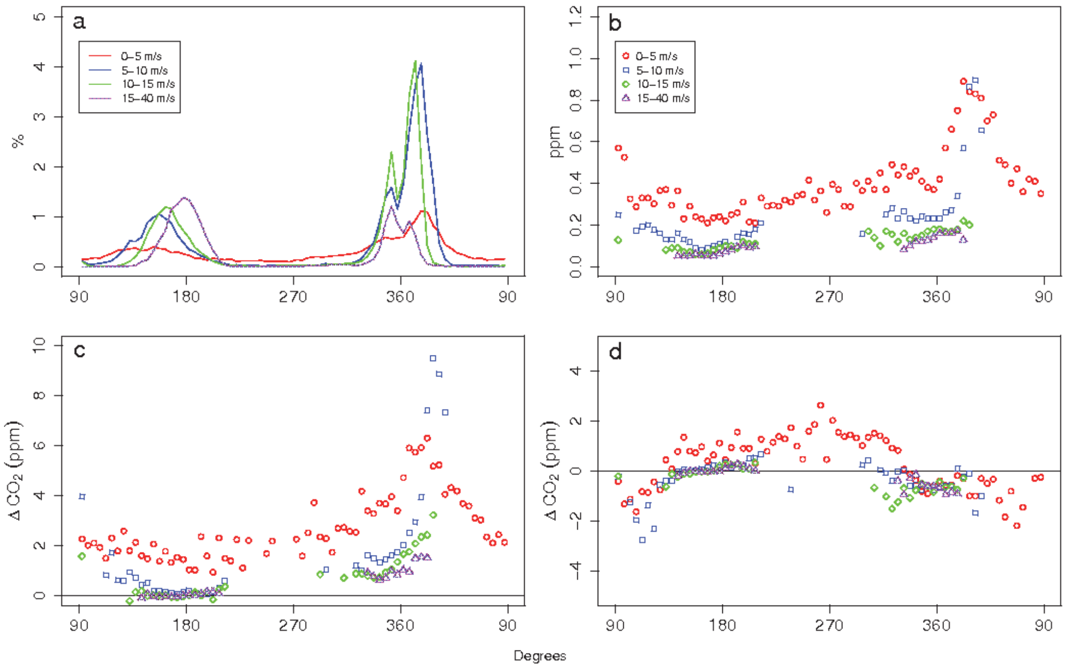

Fig. 2. Influence of wind speed and direction on CO_2 mole fractions and variability as derived from Baring Head data from 1996–2011. **(a)** Wind direction distributions for four different wind speed ranges shown as percentage of all winds in 5-degree increments. **(b)** Hourly CO_2 variability (1-sigma) as a function of wind direction for four different wind speed ranges. **(c)** Differences between night time (22:00–04:00 LST) hourly mean observed CO_2 mole fractions and interpolated steady period data for four different wind speed ranges, showing only data representing 0.05 % or greater of all wind conditions. **(d)** Same as **(c)** but for daytime (10:00–16:00 LST).

BGD
9, 15237–15277, 2012

Title Page
Abstract | Introduction
Conclusions | References
Tables | Figures
◀| |▶
◀ ▶
Back | Close
Full Screen / Esc
Printer-friendly Version
Interactive Discussion

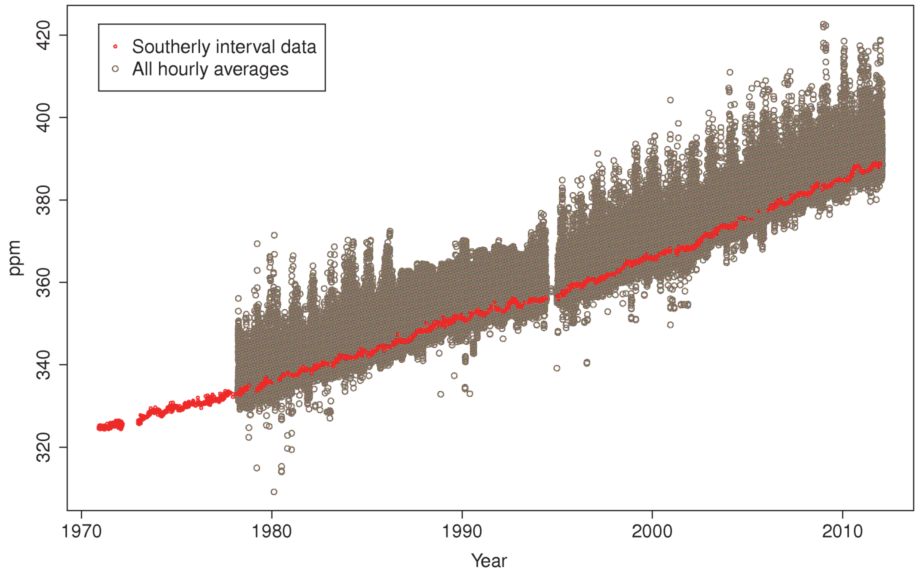

Fig. 3. Baring Head CO_2 time series, showing all hourly averages (gray) and data selected for steady periods as described in the text (red). The selected data are shown as a single average value for the entire period. The period from 1987–1994 with truncated hourly CO_2 peaks resulted from an intentional adjustment of the analyzer output range to increase sensitivity during southerly wind periods, but sacrificing measurements during locally influenced high CO_2 episodes. With the focus on the steady period data, the hourly average record was not historically scrutinized. Low CO_2 anomalies in the hourly average record prior to 2002 likely result from instrumentation problems and work is currently underway to use hand written notes to identify and filter such events out. Prior to 1978, high-rate data is not available in digital form.

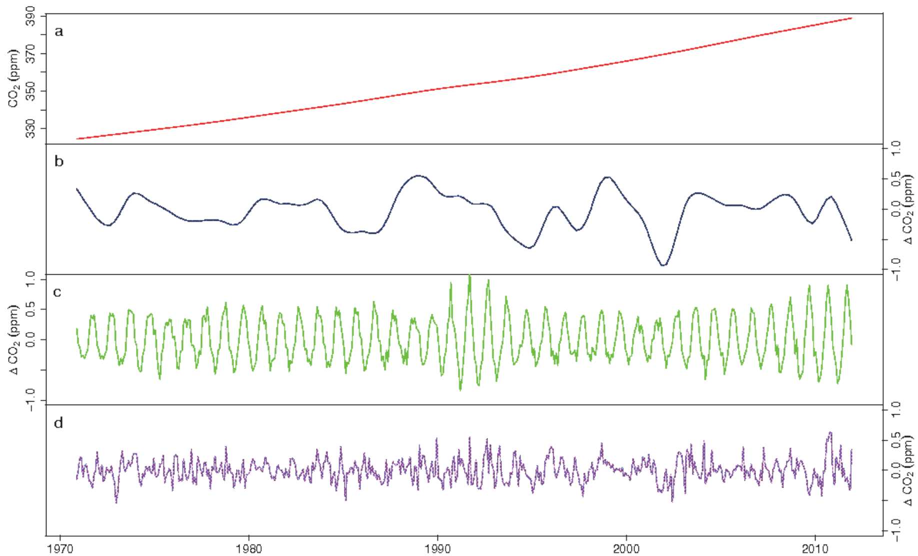

Fig. 4. Results of STL decomposition of the Baring Head steady period record. **(a)** Trend component found using 10-yr window, **(b)** interannual component found using 2-yr window, **(c)** seasonal component using a 5-yr window on monthly trends, **(d)** remainder component.

BGD

9, 15237–15277, 2012

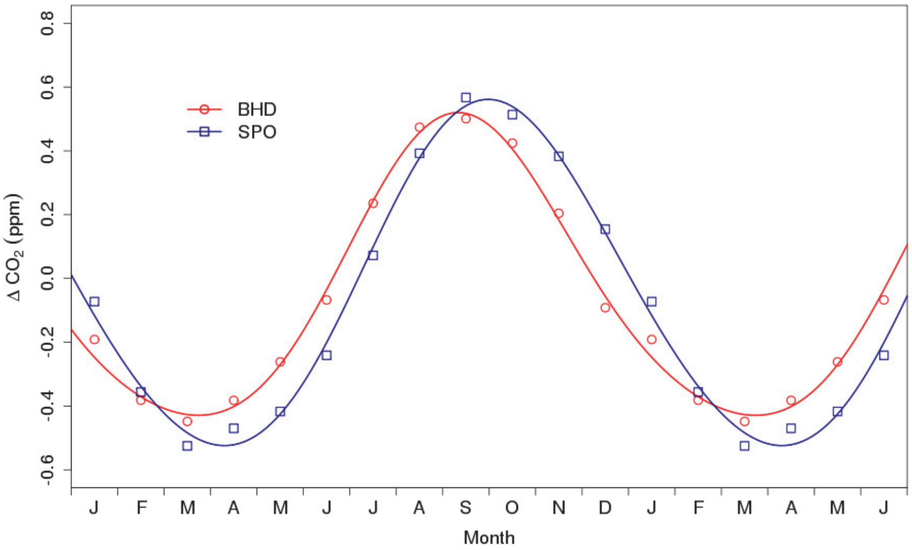

Fig. 5. Long-term average Baring Head and South Pole seasonal cycles shown as monthly means of the STL fit seasonal component (symbols) along with 2-harmonic fits to detrended monthly mean data (lines). Harmonic fits to the monthly means of the STL seasonal component are nearly identical. 18 months are shown with January–June repeated for clarity.

BGD
9, 15237–15277, 2012

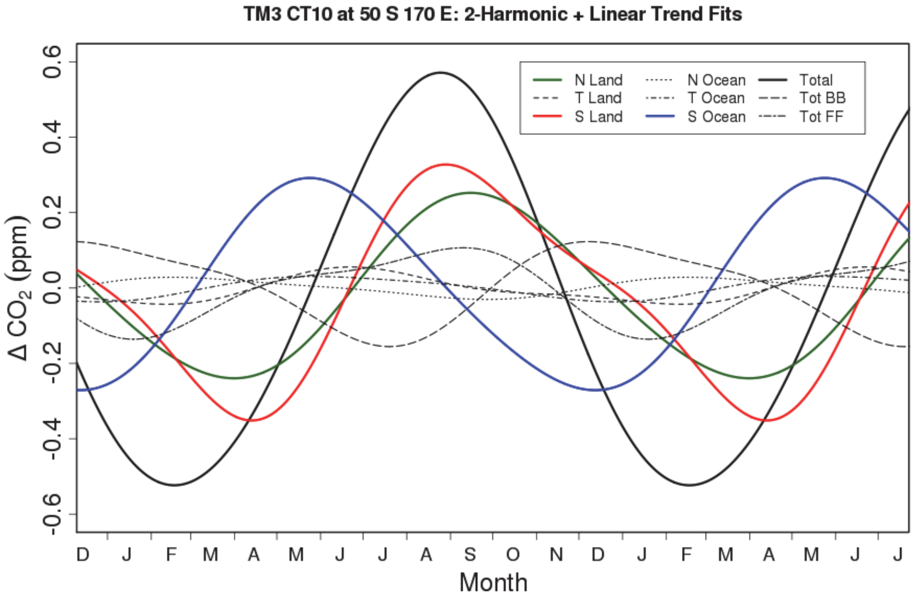

Fig. 6. Contributions to the seasonal CO_2 cycle at Baring Head as simulated by TM3 forced by CarbonTracker 2010 fluxes (Peters et al., 2007). 18 months are shown with January–June repeated for clarity. The northern (N), tropical (T), and southern (S) allocation is based on the TransCom regions (Gurney et al., 2003) with tropical divisions at approximately 15° N and 15° S. Total contributions from biomass burning (BB) and fossil-fuel emissions (FF) are also shown.

BGD
9, 15237–15277, 2012

A 39-yr atmospheric CO_2 record from Baring Head, New Zealand

B. B. Stephens et al.

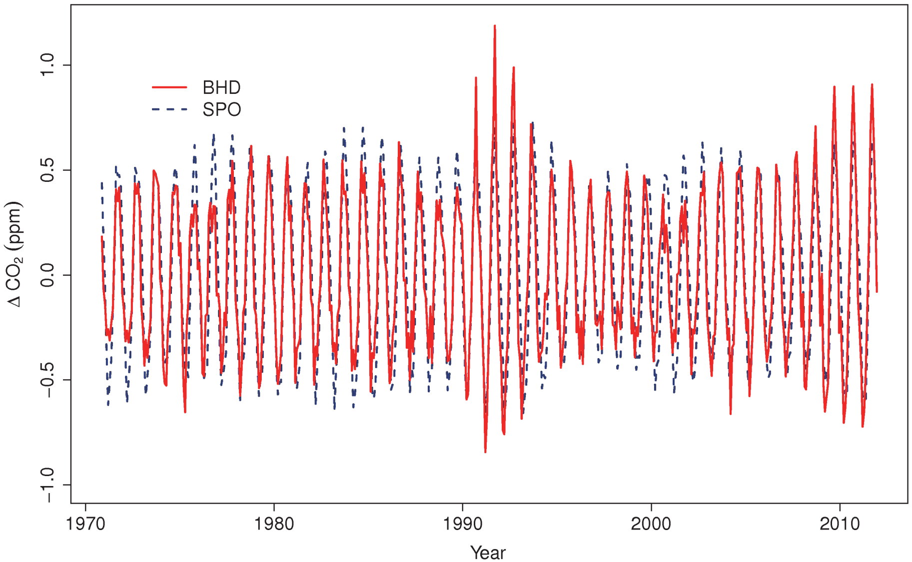

Fig. 7. Seasonal cycle components from STL decomposition of Baring Head and South Pole records. Fits used a 5-yr smoothing window on Loess fits to individual monthly time series.

BGD
9, 15237–15277, 2012

A 39-yr atmospheric CO_2 record from Baring Head, New Zealand

B. B. Stephens et al.

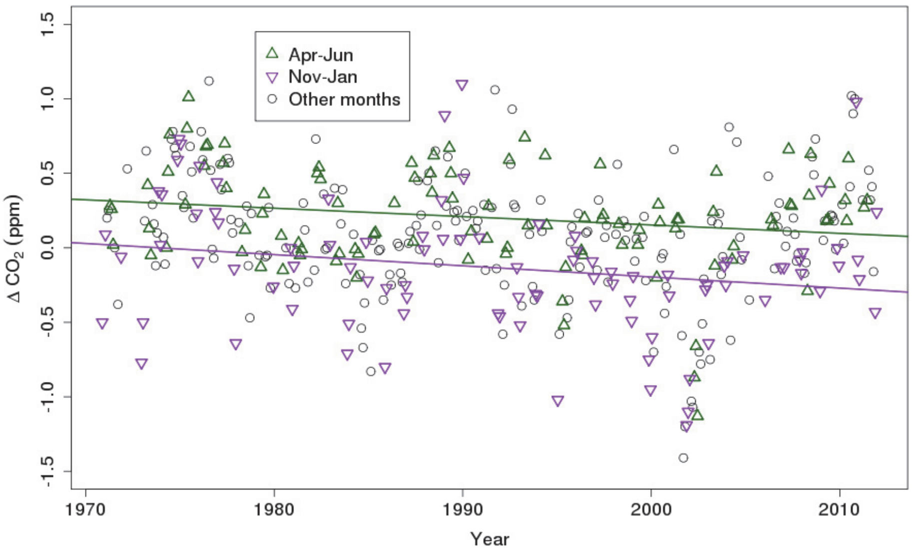

Fig. 8. Monthly mean differences between Baring Head and South Pole. Months during the peak (April–June) and trough (November–January) of the modelled influence from Southern Ocean fluxes (Fig. 6) are highlighted and fit with trend lines.

BGD
9, 15237–15277, 2012

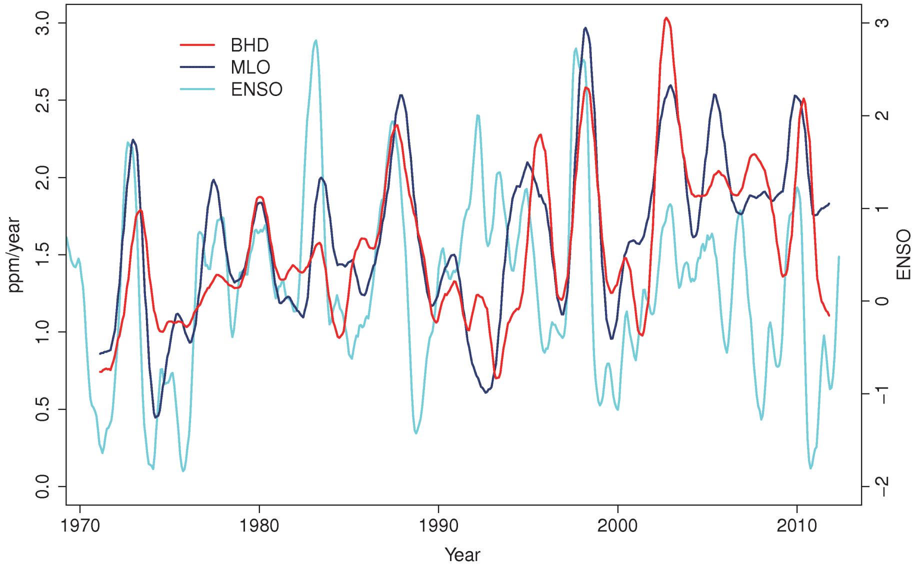

Fig. 9. Baring Head and Mauna Loa growth rate and the Multivariate ENSO Index (Wolter and Timlin, 1993). The growth rates were calculated from the month-to-month change in the sum of the trend and interannual components of the STL fits to each record (Fig. 4a, b for BHD). All three time series have been smoothed with a 5-month running mean for clarity.

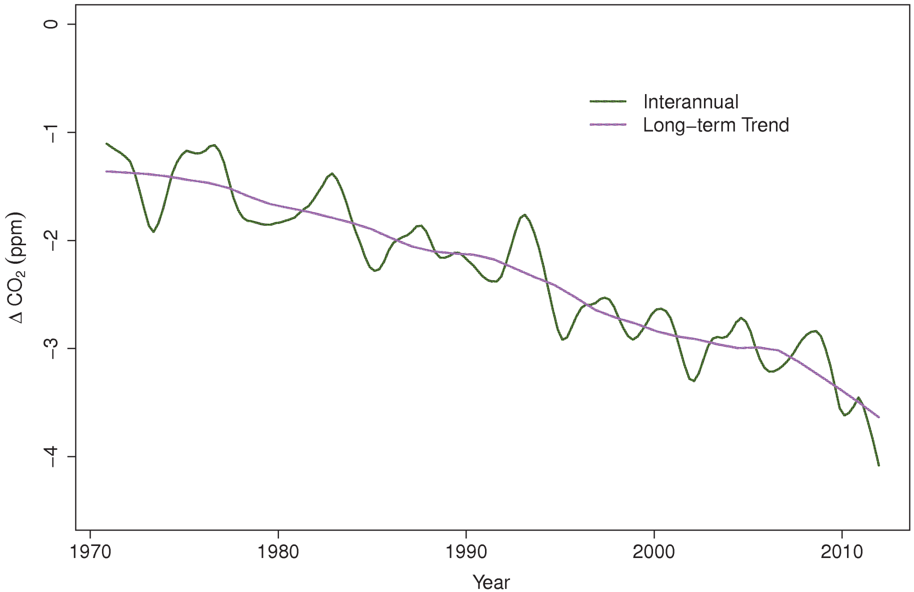

Fig. 10. BHD-MLO differences in the interannual and trend components of the STL decomposition of the Baring Head and Mauna Loa records.

BGD
9, 15237–15277, 2012

A 39-yr atmospheric CO_2 record from Baring Head, New Zealand

B. B. Stephens et al.

Title Page
Abstract | Introduction
Conclusions | References
Tables | Figures
◂ ▸
Back | Close
Full Screen / Esc
Printer-friendly Version
Interactive Discussion

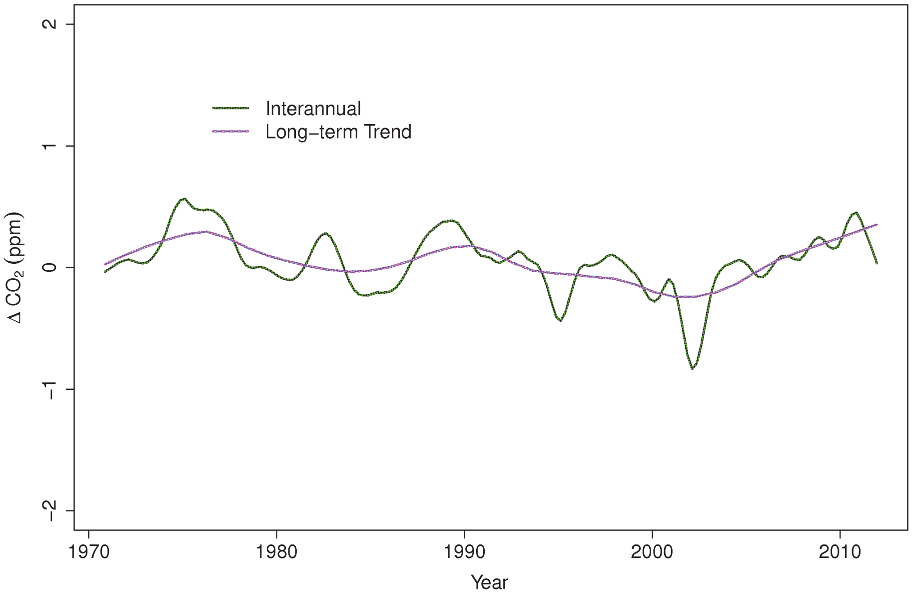

Fig. 11. BHD-SPO differences in the interannual and trend components of the STL decomposition of the Baring Head and South Pole records.

BGD
9, 15237–15277, 2012

A 39-yr atmospheric CO_2 record from Baring Head, New Zealand

B. B. Stephens et al.